



DFT studies of small rare-gas clusters

Koushiki Gupta

Department of Chemistry, University of Kalyani, Kalyani
741235, India

**Asoke P.
Chattopadhyay**

Department of Chemistry, University of Kalyani, Kalyani 741235,
India

ABSTRACT

Small rare gas clusters Rg_n ($n=3-7$) has been studied at the DFT level using a fairly large basis set (aug-cc-pV5Z) and PBELYP functional. Potential energy curves of ground states over some interatomic distances have been plotted. Binding energy and equilibrium bond distance values agree with experimental findings.

KEYWORDS

DFT, rare-gas clusters, density functionals

Introduction

In a previous paper¹ we studied rare gas dimers with a few exchange-correlation functionals in DFT procedure and presented their binding energy plots along with some other physical properties. Very few studies have been performed regarding the structure of medium-sized rare-gas clusters ($n = 3, 4, 5, 6, 7$) especially the neutral ones. The most likely reason is that the corresponding rare-gas cations are more stable than their neutral counterparts and they can be more easily produced, detected and analyzed. There are only a few results for neutral trimers so far. Three body potential for neutral He_3 has been performed by Cohen and Murrell.² Also He_3 has been studied by symmetry adopted perturbation theory (SAPT).³ He_3 bound states were calculated by variational method⁴ described in terms of atom pair co-ordinates and distributed Gaussian basis functions for zero total angular momentum. The method is also applied to calculate first vibrational levels of Ne_3 and Ar_3 cluster. On the other hand rare-gas cluster ions have received considerable attention regarding both experimental and theoretical studies. In one of the recent studies Echt et.al,⁵ measured the appearance energies of Ar_n clusters ($n \leq 30$) by electron impact of gaseous clusters and carried out quantum chemical calculations to determine the adiabatic and vertical ionization energies for cluster size upto 4 and 6 respectively. In the past few years considerable attention has been paid towards Kr_n clusters. Binding energy and structures of Kr_n^+ for $n \geq 3$ have been calculated using the dimer-in-molecule or DIM model.⁶

The structure predicted in this work was mostly based on trimeric core with a strong exception in case of Kr_4^+ . Monte Carlo simulations have also been carried out on Kr_3^+ and Kr_4^+ to investigate temperature dependent structural changes.⁷ Kalus and Paidarova⁸ constructed accurate potential energy curves for ionic krypton dimers and later extended these results towards higher cluster ions ($n = 3 - 20$) implementing coupled cluster approach. Staemmler⁹ studied the structures of small He cluster ions, upto $n = 5$ using SCF and CEPA methods. Mark and Scheier¹⁰ studied higher neutral neon clusters ($n = 90$) by electron impact ionization mass spectrometry. They confirmed the extra stability for Ne_{13} and Ne_{55} clusters having icosahedral structure. Also other two magic numbers observed viz. 21 and 75 are also observed for Ne clusters which are not seen in the case of other rare-gas clusters. Knowles et al.¹¹ proposed a new formalism for potential functions of helium cluster ions modifying the much-implemented DIM approach. Cations for medium sized Ar clusters are studied by Ikegami et

al.¹² Stable structures for these cations are found by analytical gradient method for the diatomics-in-molecules hamiltonian. Structures of all the clusters are found to be based on a trimeric core.

We have implemented some well-known density functionals to study neutral He, Ne, Ar and Kr clusters of size 3, 4, 5, 6 and 7. Different geometries of each of the clusters are studied and the respective potential energy curves are constructed.

Theory

In all the calculations, standard DFT procedure was used. In order to choose appropriate functionals for the clusters we selected He and Ne as samples and tested several functionals, namely, PBEVWN,¹³ PBELYP,¹⁴ PBEOP,^{15,16} BHHLYP.¹⁷ No other functional, except PBELYP, yielded a bound state for the above two types of clusters. Henceforth, PBELYP was accepted as a reliable one and further extended to calculation involving other geometries of all the clusters. We used aug-cc-pV5Z basis set¹⁸ throughout this work for computation. The binding energies thus obtained were corrected for basis set superposition error (BSSE) making use of the method of Boys and Bernardi.¹⁹ All the DFT computations were carried out using GAMESS-US (Sep 7, 2006 version)²⁰ suite of software package.

Results and Discussion

I. Triatomic Curves

We select the best functional from a set by testing several functionals from binding energy (B.E) and equilibrium distance (r_e) calculation of two geometries (C_{3h} and D_{3h}) of He and Ne trimer. Only the PBELYP functional was found to show a bound state for the two above mentioned trimers. Hence it was chosen for calculation of other two geometries as well as for the heavier atoms. B.E. vs. internuclear distance plots for He_3 , Ne_3 , Ar_3 and Kr_3 are presented in the Fig. 1(a)–(d).

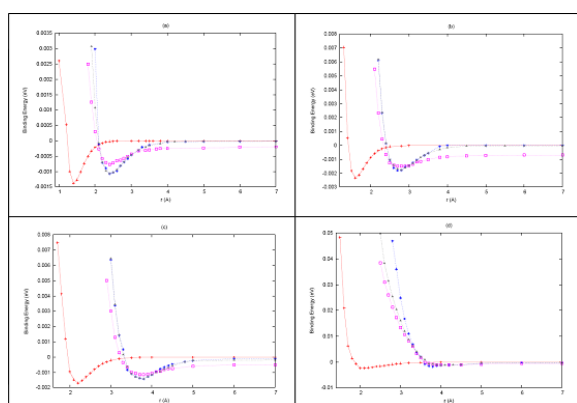
For all the triatomic clusters equilateral triangular geometry was found to be the most stable one. But the stability decreases gradually for Ar_3 and Kr_3 . Ne_3 is found to be most stable of all these species, stability being almost twice greater than that of its He counterpart. Potential curve for equilateral geometry of Kr trimer shows some dissociative nature. Both isosceles and symmetric linear geometries provide near stable curves like the equilateral triangular geometry. The stability of Kr trimer decreases abruptly from Ar and Ne. For isosceles geometry calculation is carried out at a fixed angle of 108° . As all the rare gas atoms are polarisable, at small angle repul-

sion is observed between two atoms. As a result the potential curve rises steeply. This steepness gradually decreases from He to Kr (as the interaction then belongs to soft sphere regime). The asymmetric linear structure is the least stable of all the geometries. It is seen that Ne is the most stable cluster for all the geometries. Ar and Kr trimers show markedly unstable curves with Kr trimer potential curve does not support a bound state.

Table I: Binding Energy (eV) and equilibrium bond distance (Å) of four rare gas triatomic molecules

	Binding Energy (eV)				Equilibrium Distance (Å)			
	Equi.Tri.	Asym. Linear	Iso. Tri.	Sym. Linear	Equi.Tri.	Asym. Linear	Iso. Tri.	Sym. Lin.
He	0.0014	0.00076	0.0011	0.0009	1.4	2.4	2.6	2.6
Ne	0.00234	0.00150	0.0018	0.0018	1.6	2.8	2.7	2.8
Ar	0.0017	0.00116	0.0014	0.0014	2.2	3.7	3.8	3.8
Kr	0.00073	0.0015	0.0017	0.00099	1.9	3.9	3.8	3.9

Fig. 1. Binding Energy (eV) vs. equilibrium distance (Å) plot for different geometries of (a)



(a) He₃, (b) Ne₃, (c) Ar₃, (d) Kr₃. [Blue line with star denotes isosceles triangle, grey line with filled triangles denotes symmetric linear, red line with crosses denotes equilateral triangle and pink line with squares denotes asymmetric linear geometries for all four figures.]

II. Tetrameric Curves

In this case also we choose the PBELYP functional from a set of many as it yielded the most stable states for the tetramers. B.E. (eV) vs. internuclear distance (Å) plots for different geometries of He₄, Ne₄, Ar₄ and Kr₄ are presented in the Fig. 2(a)–(d).

For He₄, Ne₄ and Ar₄, tetrahedral geometry is the most stable one. For He tetramers all the geometries provide a stable potential curve with well-defined minima. As observed for the trimers, in this case also Ne₄ is the most stable of all clusters. Stability of Ne is almost ten times greater than that of He tetramers. Also, for Ne₄, symmetric linear geometry provides a much more stable state compared to its He counterpart. Square planar and tetrahedral geometries show almost equal minima for Ne₄. The observation that Ne trimers and tetramers are more stable than clusters of other rare gas atoms deserves comment. We are investigating this issue in some detail but probably the effect arises from complex interplay between attraction and repulsion in the increasingly polarisable electron cloud going from He to Kr. For Ar₄, all the geometries provide a well-defined bound state and shows nearly same stability as that of Ne. Again stability decreases abruptly for Kr tetramers. But in a marked contrast from other tetramers, for Kr₄ symmetric linear geometry is the most stable of all geometries, while square planar and tetrahedral geometry represent less strongly bound potential states. Basis set superposition error increases in magnitude from He to Kr but does not have any significant effect on the binding energy of the tetramers (as is quite expected for rare-gas clusters which are nearly ideal

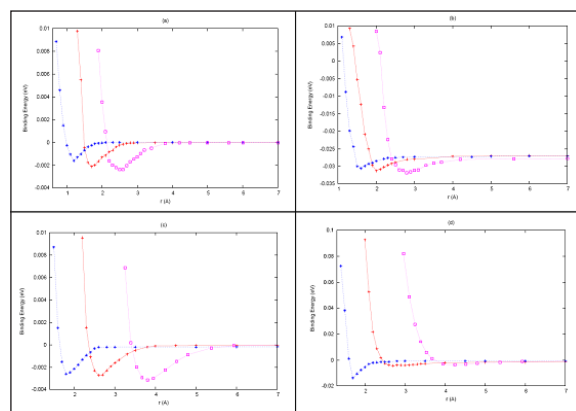
The basis set superposition error is calculated for all geometries but it seems to have negligible effect on the total energies of the systems. The magnitude of BSSE increases from He to Kr trimer (16.6 μeV for He and 42 μeV for Kr trimer, 1 μeV = 10⁻⁶ eV) but still it does not contribute significantly (in order of microhartrees) towards the binding energies of the clusters.

non-interacting systems).

Table 2. Binding Energy (eV) and equilibrium bond distance (Å) of four rare gas tetrameric molecules.

	Binding energy (eV)			Equilibrium Distance (Å)		
	Sq. Planar	Tetrahedral	Sym. Linear	Sq. Planar	Tetrahedral	Sym. Linear
He	0.0021	0.0024	0.0016	1.7	2.5	1.2
Ne	0.0312	0.0318	0.0305	2.0	2.8	1.6
Ar	0.0027	0.0031	0.0026	2.6	3.81	1.8
Kr	0.0044	0.0037	0.0137	2.7	4.24	1.7

Fig 2. Binding Energy (eV) vs. equilibrium distance (Å) plot for different geometries of (a)



He₄, (b) Ne₄, (c) Ar₄ and (d) Kr₄. [Blue line with star denotes DYh, red line with cross denotes D_{4h} and pink line with squares denotes Td geometry for all four figures.]

III. Pentatomic Curves

We select the best functional from a set of few well-known exchange-correlation functionals in the DFT formalism by testing several functionals from binding energy (B.E) and equilibrium distance (r_e) calculation of trigonal bi-pyramidal geometry of He and Ne pentamer. Only the PBELYP functional was found to show a bound state for the two above mentioned pentamers. Thus it was chosen for calculation of other two geometries (C_{4v} and D_{5h}) and was also implemented for the heavier atoms. B.E. vs. r plots for He₅, Ne₅, Ar₅ and Kr₅ are presented in the Fig. 3(a)–(d).

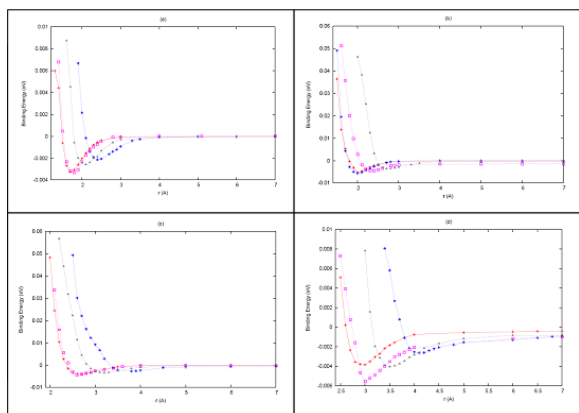
For all the pentamers tetragonal bipyramidal (TBP) and C_{4v} geometry are the most stable. For He pentamer, TBP and C_{4v} geometry provide almost identical state with a well-defined potential minima. Binding energies for these two geometries are nearly comparable, symmetric linear and D_{5h} geometries represent curves with much less well-depth. The former (i.e., D_{∞h}) is the least stable among the four geometries. For Ne complex

again TBP and the C_{4V} yielded very similar curves but the stability increases almost two-fold from that of He_5 . On the other hand the remaining two geometries represented much shallower curves, and well-depth decreased from that of He_5 . Ar_5 is less stable than Ne_5 , but more stable as compared to He_5 . $D_{\infty h}$ and D_{5h} potentials show shallow states with binding energies almost comparable with the other two geometries. On the other hand, all the geometries for Kr_5 represent exceptionally stable states with remarkably well-defined potential minima (similar to those of He_5). In this case, in marked contrast with the previous three clusters (He_5 , Ne_5 and Ar_5), TBP and C_{4V} geometries are shown to yield distinctly separate potential curves, C_{4V} being the most stable (stability almost the same as Ne_5). For Kr_5 , TBP and D_{5h} geometries have nearly identical potential minima (0.0038 and 0.0040 eV respectively), D_{5h} being a little less stable than Ar_5 and nearly equal to Ne_5 . Linear symmetric structure is again the most unstable of all four geometries studied. Binding energy for this geometry is less than that of Ne_5 but comparable to He_5 and Ar_5 . BSSE have been calculated for all the clusters (keeping one pseudo atom). It seems to have no significant effect on the total energy as well as the binding energy of the pentamers. This is very similar to what was observed in the case of Rg_3 and Rg_4 .

Table 3. Binding Energy (eV) and equilibrium bond distance (A) of four rare gas pentatomic molecules.

	Binding Energy (eV)				Equilibrium Distance (A)			
	TBP	D_{5h}	C_{4V}	$D_{\infty h}$	TBP	D_{5h}	C_{4V}	$D_{\infty h}$
He	0.0032	0.0026	0.0033	0.0021	1.7	2.1	1.8	2.4
Ne	0.0053	0.0045	0.0057	0.0036	2.0	2.3	2.0	2.7
Ar	0.0040	0.0034	0.0044	0.0027	2.7	3.2	2.6	3.8
Kr	0.0038	0.0040	0.0055	0.0026	3.0	3.5	3.0	4.2

Fig. 3. Binding Energy Plot for different geometries of (a) He_5 , (b) Ne_5 , (c) Ar_5 and (d) Kr_5 .



[Blue line with star denotes $D_{\infty h}$ geometry, grey line with filled triangle denotes D_{5h} geometry, red line with cross denotes TBP and pink line with squares denotes C_{4V} geometry for all four figures.]

IV. Hexatomic Curves

On the basis of calculations on the equilibrium bond distance (r_e , Å) and binding energy (B.E., eV) studies of the homonuclear rare gas hexatomic molecules (He_6 and Ne_6), PBELYP functional was selected to study the geometries of other two clusters. B.E. vs. r plots for He_6 , Ne_6 , Ar_6 and Kr_6 are represented in the Fig. 4(a)–(d).

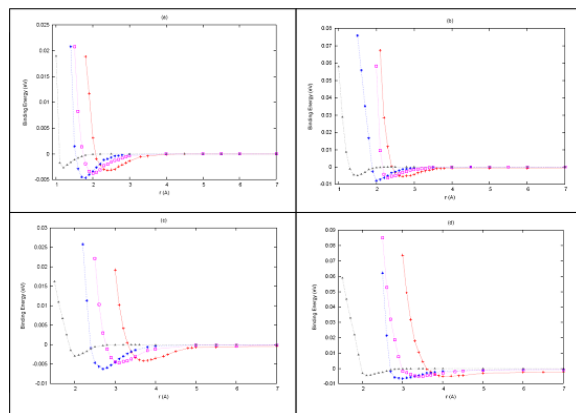
For He_6 , all the geometries provide a stable potential state though the curves show some shallow nature. Octahedral structure is the most stable geometry and the corresponding curve shows considerable well-depth (B.E.=0.0046 eV). The other three geometries (D_{6h} , C_{5V} and $D_{\infty h}$) represents near-

ly similar curves with more or less equal binding energy (but different equilibrium distances) with symmetric linear structure shows a sharp potential curve. For Ne_6 also octahedral geometry provides the stablest structure. In this case binding energy from the O_h curve is almost 1.7 times (0.0079 eV) that of O_h (He_6). D_{6h} curve does not possess a sharp potential minimum, showing some dissociative nature. All the curves are lower in energy than He_6 , as it was observed in case of Rg_5 . For Ar_6 , all the geometries represent stable potential curves with pretty high well-depths. Binding energy corresponding the O_h structure though less than Ne_6 , but is much higher than He_6 . D_{6h} and C_{5V} geometries have almost equal binding energy (0.0041 and 0.0045 eV). Linear symmetric curve ($D_{\infty h}$) again represents a sharp nature much like that of Ne_6 (B.E. though higher than Ne_6). Thus it is seen that, for Rg_6 too, Ne_6 is the most stable of the four clusters similar to that of Rg_4 and Rg_5 . Stability of the clusters decrease gradually as we move from Ne to Ar and Kr. For Kr, none of the geometries seem to represent a clear bound state. All the curves are extremely shallow with D_{6h} and C_{5V} possessing no sharp potential minima. Octahedral is the most stable of the four and the corresponding binding energy is nearly equal to Ne_6 . D_{6h} geometry represents potential state near to the dissociation limit. Symmetric linear geometry, as a marked contrast from He_6 , Ne_6 and Ar_6 , does not show a sharp nature of the potential curve, rather it observes a state which shows some dissociative nature. Again BSSE effect does not influence the binding energy of the systems (modifies in the order of microeV).

Table 4. Binding Energy (eV) and equilibrium bond distance (A) of four rare gas hexatomic molecules.

	Binding Energy (eV)				Equilibrium Distance (A)			
	O_h	D_{6h}	C_{5V}	$D_{\infty h}$	O_h	D_{6h}	C_{5V}	$D_{\infty h}$
He	0.0046	0.0032	0.0037	0.0027	1.8	2.4	2.0	1.2
Ne	0.0079	0.0054	0.0062	0.0049	2.0	2.7	2.3	1.5
Ar	0.0061	0.0041	0.0045	0.0029	2.7	3.7	3.1	2.0
Kr	0.0065	0.0053	0.0052	0.0046	3.0	4.0	3.4	2.1

Fig. 4. Binding Energy Plot for different geometries of (a) He_6 , (b) Ne_6 , (c) Ar_6 and (d) Kr_6 .



[Blue line with star denotes O_h geometry, grey line with filled triangle denotes D_{6h} geometry, red line with cross denotes D_{6h} geometry and pink line with square denotes C_{5V} geometry for all four figures.]

V. Heptatomic Curves

For rare gas heptamers also we choose the PBELYP density functional based on the equilibrium bond distance (r_e , Å) and binding energy (B.E., eV) studies of He_7 and Ne_7 . B.E. vs. r plots for He_7 , Ne_7 , Ar_7 and Kr_7 are represented in the Fig. 5(a)–(d).

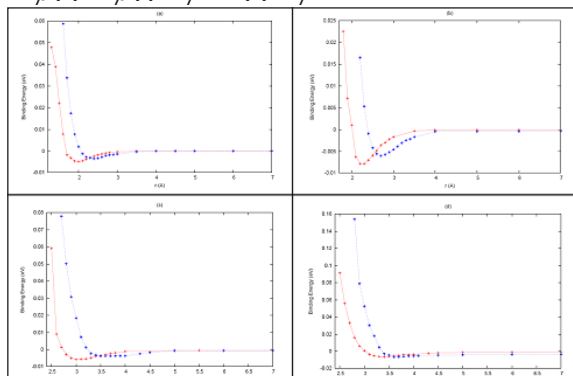
Only two geometries (D_{5h} i.e. pentagonal bipyramid and C_{6V})

are studied for all Rg_7 clusters. For He_7 , D_{5h} potential curve shows a clear bound state though it is much shallow than the previously studied He clusters. The binding energies of the two geometries are comparable but C_{6v} is the less stable one and shows some dissociative nature. For Ne_7 , D_{5h} geometry shows a sharp potential curve with considerable well-depth and stability is about 1.6 times greater than He (thus the observed pattern of the Ne cluster being most stable among the four is maintained here also). C_{6v} is also a much stabler geometry for Ne compared to that of He and represents a deep curve with binding energy of 0.0060 eV which is about 1.7 times that of He_7 . In case of Ar_7 , curves more or less reflect the nature of He_7 (binding energy though less than He). Stability decreases markedly from that of Ne_7 for both the geometries with C_{6v} structure again showing dissociative nature to some extent. For Kr_7 , both the geometries represent almost overlapping potentials and the curves are too shallow to support a bound state. BSSE effects are again insignificant in contributing towards binding energies of the clusters as was observed for Rg_4 , Rg_5 and Rg_6 .

Table 5: Binding Energy (eV) and equilibrium bond distance (Å) of four rare gas hepta-atomic molecules.

	Binding Energy (eV)		Equilibrium Distance (Å)	
	D_{5h}	C_{6v}	D_{5h}	C_{6v}
He	0.0048	0.0036	2.0	2.4
Ne	0.0079	0.0060	2.3	2.7
Ar	0.0058	0.0038	3.0	3.5
Kr	0.0063	0.0068	3.4	3.6

Fig. 5. Binding Energy Plot for different geometries of (a) He_7 , (b) Ne_7 , (c) Ar_7 and (d) Kr_7 .



[Blue line with star denotes C_{6v} geometry, and red line with cross denotes D_{5h} geometry for all four figures.]

Conclusion

Electronic structure calculations were carried out on neutral clusters of rare gas atoms of the type Rg_n where $n = 3, 4, 5, 6, 7$ and $Rg = He, Ne, Ar$ and Kr . The basis set used was aug-ccpV5Z of Dunning et al.¹⁷ throughout the work. We used PBELYP for all the clusters. Also the binding energy values were corrected for basis set superposition error implementing the method of Boys and Bernardi¹⁸ but BSSE does not seem to have any significant effect on them. For Rg_3 equilateral triangle and for Rg_4 tetrahedral geometry is most stable. In a similar way the tetragonal bipyramidal and octahedral geometry was found to be the most stable one for the penta and hexamers respectively. The stability order for all the clusters is $He < Ne > Ar >> Kr$. For higher clusters, the lack of experimental data precludes comparison with the latter. Lack of experimental and theoretical data for the above mentioned clusters prevent comparison of our results with them. Most of the previous theoretical studies deal with rare gas trimer and tetramers positively charged ions as they are more abundant and stable in nature. Further work is needed to establish the optimum choice of basis set and functional for these systems.

Acknowledgement

The authors wish to thank the DST-FIST and UGC-SAP (DRS) grant to the Department of Chemistry, University of Kalyani and DST PURSE grant to the Faculty of Science, University of Kalyani for infrastructural support, esp. regarding computational facility. The authors are especially grateful to Prof. S. K. Pati, Theoretical Sciences Unit, J.N.C.A.S.R., Bangalore, India for hospitality and computational resources.

REFERENCES

- 1 K. Gupta and A. P. Chattopadhyay, *Galaxy Int. Interdisc. Res. J.* 3, 54 (2015)
- 2 M. J. Cohen and J. N. Murrell, *Chem. Phys. Lett.* 260, 371 (1996).
- 3 V. F. Lotrich and K. Szalewicz, *J. Chem. Phys.* 112, 112 (2000).
- 4 T. Gonzalez-Lezana, J. Rubayo-Soneira, S. Miret-Artes, F.A. Gianturco, G. Delgado-Barrio and P. Villarreal, *J. Chem. Phys.* 110, 9000 (1999).
- 5 O. Echt, T. Fiegele, M. Rummele, M. Probst, S. Matt-Leubner, J. Urban, P. Mach, J. Leszczynski, P. Scheier and T. D. Mark, *J. Chem. Phys.* 123, 084313 (2005).
- 6 F. O. Ellison, *J. Am. Chem. Soc.* 85, 3540 (1963).
- 7 R. Kalus, D. Hrivnak and A. Vitek, *Chem. Phys.* 325, 278 (2006).
- 8 R. Kalus, I. Paidarova, D. Hrivnak, P. Paska and F. X. Gadea, *Chem. Phys.* 294, 141 (2003).
- 9 V. Staemmler, *Z. Phys. D* 16, 219 (1990).
- 10 T. D. Mark and P. Scheier, *Chem. Phys. Lett.* 137, 245 (1987).
- 11 P. J. Knowles, J. N. Murrell and E. J. Hodge, *Mol. Phys.* 85, 243 (1995).
- 12 T. Ikegami, T. Kondow and S. Iwata, *J. Chem. Phys.* 98, 3038 (1993).
- 13 S. H. Vosko, L. Wilk and M. Nusair, *Can. J. Phys.* 58, 1200 (1980).
- 14 C. Lee, W. Yang and R. G. Parr, *Phys. Rev. B* 37, 785 (1988).
- 15 J. P. Perdew, K. Burke and M. Ernzerhof, *Phys. Rev. Lett.* 77, 3865 (1996).
- 16 T. Tsuneda, T. Suzumura and K. Hirao, *J. Chem. Phys.* 110, 10664 (1999).
- 17 A. D. Becke, *J. Chem. Phys.* 98, 1372 (1993).
- 18 T. H. Dunning, Jr., *J. Chem. Phys.* 90, 1007 (1989).
- 19 S. F. Boys and F. Bernardi, *Mol. Phys.* 19, 553 (1970).
- 20 M. W. Schmidt et al., *J. Comput. Chem.* 14, 1347 (1993).